

Cross section for production of the metastable H(2S) state in proton collisions with atomic hydrogen*

Y. P. Chong[†] and W. L. Fite

Department of Physics and Astronomy, University of Pittsburgh, Pittsburgh, Pennsylvania 15260

(Received 29 July 1976)

Cross sections for production of the metastable H(2S) state in collisions of 6–25-keV protons with atomic hydrogen have been measured in a modulated crossed-beam experiment. The metastable states excited through the process $H^+ + H \rightarrow H^+ + H(2S)$ (direct excitation) and $H^+ + H \rightarrow H(2S) + H^+$ (charge transfer) were quenched in a weak electric field applied at the collision region. The emitted Lyman- α radiation was detected in a direction perpendicular to the plane of the crossed beams. The processes were separable since the direct excitation signals saturated well before the charge transfer signals did as the quench field was increased. The present values were normalized to the absolute total cross section for H(2P) production measured by Kondow *et al.* The charge-transfer cross sections are in satisfactory agreement with the measurements of Morgan *et al.* and Bayfield except at 6 keV, where their values also begin to differ. The direct-excitation cross section differs in shape from the only other measurement of Morgan *et al.*, but agrees in absolute magnitude when normalization uncertainties are included. The coupled-state calculations of Cheshire *et al.* using a pseudostate expansion show good agreement with the present results, indicating the importance of the inclusion of molecular features at small internuclear separations.

I. INTRODUCTION

The cross sections for production of the metastable H(2S) state in proton collisions with atomic hydrogen through the processes

$$H^+ + H \rightarrow H^+ + H(2S) \quad (\text{direct excitation}) \quad (1)$$

and

$$H^+ + H \rightarrow H(2S) + H^+ \quad (\text{charge transfer}) \quad (2)$$

have been measured in the proton energy range 6–25 keV. Extensive theoretical studies involving numerous approximations^{1–24} have been made for these basic atomic-collision processes with a large variation in the predicted results. Scattering of protons in the low-keV range by atomic hydrogen is of particular interest in this case because (i) the Born approximation appears invalid below 100 keV, (ii) the inclusion of charge-transfer reaction channels in theoretical calculations gives rise to structure in the cross sections in this energy range, and (iii) the effect of including pseudostates in close-coupling calculations to simulate molecular features at small internuclear separations can be evaluated.

The first measurements on the charge-transfer process (2) were made by Ryding *et al.*²⁵ in 1966 for protons of 40–200 keV. This was followed by the experiments of Bayfield²⁶ for protons in the range 3–70 keV. Both these experiments employed the beam furnace-gas-target method which did not permit measurement of the direct-excitation process (1). The more sophisticated modulated crossed-beam techniques, which are capable of yielding the cross section for the direct-excitation

process (1) as well as for the charge-transfer process (2), were then applied independently and concurrently at Queen's University Belfast and in this laboratory. Although similar in some respects, the experiment of Morgan *et al.*²⁷ and the present study differ in a number of significant ways. The present charge-transfer cross sections are in satisfactory agreement with the measurements of Morgan *et al.*²⁷ and of Bayfield,²⁶ except at 6 keV where their results also begin to differ. The direct-excitation cross section differs somewhat in shape from the measurement of Morgan *et al.*, but the apparent differences in magnitude may be insignificant in view of normalization uncertainties.

II. EXPERIMENTAL APPROACH

The metastable H(2S) atoms produced through processes (1) and (2) at the intersection point of the crossed proton and H-atom beams were detected by quenching in an electric field and observing the resulting Lyman- α radiation with a photomultiplier. The field was applied at the crossed-beam region in a direction parallel to the atomic-beam axis. The lifetime τ of a metastable H(2S) atom in an external electrostatic field has been derived by Bethe and Salpeter²⁸ in a weak-field time-independent perturbation theory as

$$\tau(\xi) = \tau_{2P} \left(1 + \frac{4\xi^2}{[1 - (1 + 4\xi^2)^{1/2}]^2} \right), \quad (3)$$

where τ_{2P} is the field-free lifetime (1.6×10^{-9} sec) of the 2P state and ξ is the ratio of the Stark-effect splitting to the field-free Lamb-shift splitting:

$$\xi = \sqrt{3}E_q e a_0 / L. \quad (4)$$

Here L is the Lamb shift, a_0 the Bohr radius, and e the electronic charge. Numerically ξ is about $E_q/475$, where E_q is the quenching field in V/cm. The field dependence of τ given by Eq. (3) has been experimentally verified by Sellin²⁹ in his studies on H(2S) production and extinction.

Since atoms excited into the $2P$ state were de-excited within the interaction region with spontaneous emission of Lyman- α radiation, it was necessary to measure the signal $S_1(T)$ at zero quench field, T being the temperature of the H atoms (denoted by subscript 1). The relatively long lifetime ($\frac{1}{8}$ sec)³⁰ of the field-free H(2S) atoms enabled them to leave the beam interaction region without deexcitation. When the quench field was turned on, the photon signal increased by an amount $S_1^M(T)$ which represented the induced decay of the metastable atoms. The technique applied in this laboratory to study the processes (1) and (2) simultaneously was to measure the ratio $R_1 = S_1^M(T)/S_1(T)$ as a function of quench-field voltage V_q . The metastable atoms produced through direct excitation traveled at thermal velocities (10^6 cm/sec) so that their quenched signals saturated well before those from the fast metastables (10^8 cm/sec) excited through charge transfer. The fast metastables required a stronger quench field to reduce their lifetimes sufficiently for decay to occur within the detector's field of view. The processes of direct excitation and charge transfer were therefore separable.

III. EXPERIMENTAL APPARATUS

A. Basic setup

The basic experimental apparatus is similar to that used previously in this laboratory,^{31,32} except that a titanium getter pump replaced the cryopump utilized previously to provide an ultrahigh vacuum in the beam crossing region.

Atomic hydrogen was produced by thermal

dissociation of hydrogen molecules in a joule-heated tubular furnace rolled from tungsten foil. A beam effused through a 1-mm-diam aperture in the furnace located in the first of three differentially-pumped vacuum chambers. A rotating chopper wheel modulated the beam at 270 Hz in the second chamber before it entered the third chamber and then into the getter-pumped region (chamber 5) where it was crossed at 90° by a proton beam. After emerging from chamber 5 the modulated beam was fractionally ionized by electrons of 100-eV energy. The ions were analyzed with a quadrupole mass filter in order to determine the dissociation fraction D of the hydrogen beam, given by³²

$$D = \frac{1}{1 + 0.93(s_2^{\ddagger}/s_1^{\ddagger})}, \quad (5)$$

where s_1^{\ddagger} and s_2^{\ddagger} are the detected relative atomic and molecular ion intensities. D was normally between 0.7 and 0.8. The furnace temperature was directly measured with an optical pyrometer and corrected for the presence of the chopper wheel and restrictive apertures along the viewing direction.

Hydrogen ions produced in an ion source by electron-impact ionization of H_2 were accelerated and focused into a beam by an electrostatic-quadrupole lens pair for entry into a 90° -sector magnetic field where the beam was mass analyzed. The analyzed proton beam was guided by deflector plates into an einzel lens which focused it to pass through the modulated beam as shown in Fig. 1. Practically all the protons were collected in a deep Faraday cup having an entrance aperture smaller than the height of the neutral beam at the collision region. The rest of the protons which had passed through close to the edges of the hydrogen beam were collected by an outer concentric collector. The ratio of the proton current at the outer collector to that at the central collector was normally 10^{-3} . Thus,

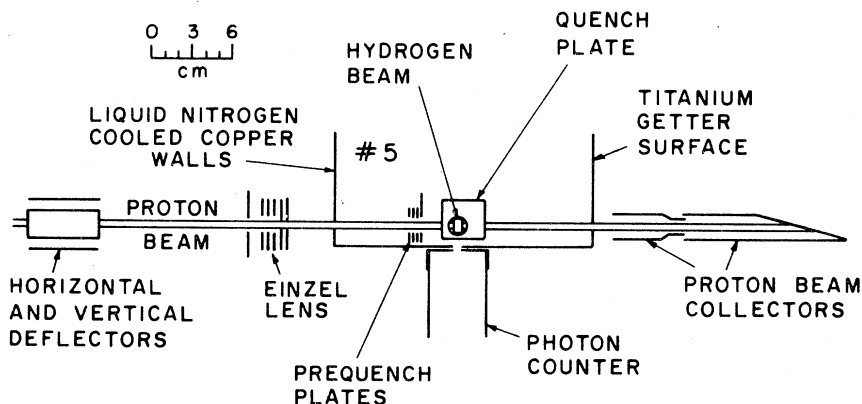


FIG. 1. Experimental apparatus for steering, focusing, defining, and collecting the proton beam.

all the protons were sure to have passed through the neutral beam. In order to suppress slow secondary electrons emitted from surfaces by proton impact, the central collector was biased at +25 V through a current-measuring electrometer, while the outer collector was grounded through another electrometer. The maximum proton current was 3×10^{-7} A.

The background gas pressure at the interaction region was reduced significantly by a titanium getter pump. Titanium evaporated from titanium-molybdenum filaments was condensed on the inner walls of a liquid-nitrogen-cooled container to form a gettering surface. A flash duration of 10 min deposited sufficient titanium to provide pumping for about 5 h. The background gas pressure at the crossed-beam region was estimated at 4×10^{-9} Torr.

B. Photon detection

The Lyman- α detector employed in this experiment consisted of a photomultiplier tube (EMR 541J-08-18) preceded by a dry molecular-oxygen filter. The sensitive range of the photomultiplier lies between 1050 and 1600 Å, while molecular oxygen has a sharp narrow window near the Lyman- α line.³³⁻³⁷ The detector located outside chamber 5 viewed the interaction region in the perpendicular direction to the plane of the crossed beams as shown in Fig. 2. Mounted on a slider, it was moved away from its aligned position before each titanium flash in order to avoid surface con-

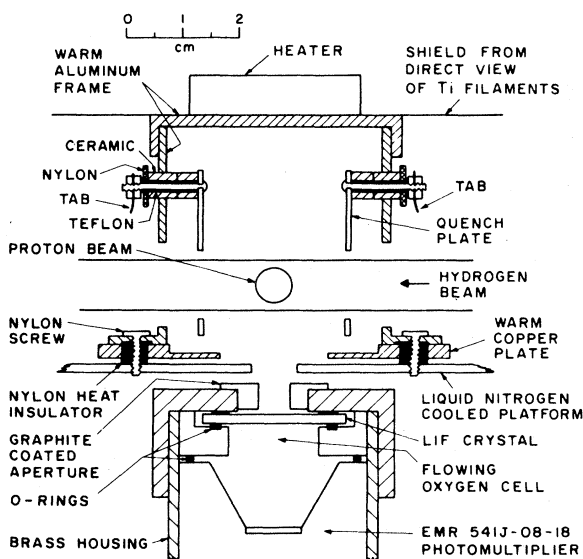


FIG. 2. Cross-sectional view of the heated quench-plate assembly and the oxygen filter of the photon detector, viewing the interaction region.

tamination of the viewing window.

A synchronous single-photon counting method was used to measure the intensity of the Lyman- α signals. A pair of phase-locked scalers were gated by the chopper-wheel reference signal, so that one scaler (A) recorded the output N_A when the H atom beam was on, while the other (B) recorded the output N_B when the proton beam passed through only the residual gas in chamber 5. The value $N_A - N_B$ gives the intensity S of the desired signal. The ratio S/N_B , indicative of the signal-to-background ratio, was greatly improved by the getter pump, reaching 4–10 immediately after a flash from 0.2 to 0.6 before the flash. As time progressed, the ratio gradually decreased to about 1.5 when another flash was made.

C. Quench field

The electrostatic field was provided by applying potentials of $+\frac{1}{2}V_q$ and $-\frac{1}{2}V_q$ to a pair of gold-plated parallel plates with circular apertures to enable passage of the neutral beam. The proton beam traversed the region of zero potential midway in between the plates. In order to determine the effect of the apertures on the field strength, the potential field distribution was measured for a scale model by means of an electrolytic plotting tank. The field strength at the crossed-beam position was found to be 0.75 times the voltage difference divided by the plate separation and varied less than 6% across the field of view. To ensure that only the desired Lyman- α radiation directly from the beam interaction point was being observed, nearby surfaces which could reflect radiation into the detector were coated with colloidal graphite.

The quench plates were required to be maintained at room temperature to prevent formation of ice layers and accumulation of local charges from scattered ions, etc., which would produce higher fields than desired. Prior to installation of the heating system, measurements of the metastable signals gave extremely low values accompanied by rather large fluctuations. This suggested quenching of the metastables even when no voltages were applied to the quench plates. The possible causes were (1) a residual magnetic field, (2) a residual electric field, and (3) collisional quenching of the metastables by residual gases. A residual magnetic field was unlikely since none of the apparatus in chamber 5 were constructed from magnetic material. Moreover, a field strength of 575 G^{38,39} is required in order to quench metastables by hyperfine level crossing between the $2S_{1/2}$ and $2P_{1/2}$ states. The dominant collisional quenching is by water vapor with a cross section of 10^{-13} cm² determined by Fite *et al.*⁴⁰ For water

vapor of number density 10^8 molecules/cm³ and metastable atoms moving with a thermal velocity of 8×10^5 cm/sec, the decay rate is only about 10 per sec. This rate is 300 times less than the decay rate induced by an electric field of 1 V/cm. From these considerations, a residual electric field from charged ice was thought to be the most likely cause. A local heated-environment system shown in Fig. 2 was found to function well, and the quenched signals were then found to increase significantly with a reduction of fluctuations. The temperature of the heated system was near room temperature and was monitored with a suitably placed iron-constantan thermocouple which also monitored for prevention of overheating the system during each flash. The quench plates and beam intersection region were shielded to avoid direct exposure to the titanium filaments.

D. Prequench field

A prequench field, applied close to the quench plates (Fig. 1) before the proton beam entered the beam intersection region, reduced strongly the quenched photon signal arising from the background. As the protons travel from the magnet exit towards the collision region, they undergo

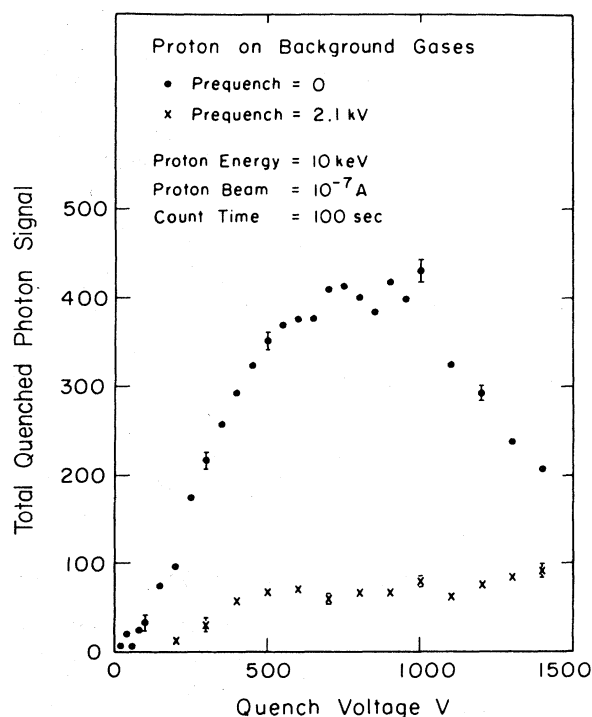


FIG. 3. Experimental determination of the quenching of metastables present in the proton beam by the prequench field: ●, zero prequench; ×, prequench=2.1 kV.

charge-transfer collisions with background gas to form metastable atoms which move along together with the proton beam. The prequench field quenched a large fraction of these metastables as shown in Fig. 3. Since beam modulation and phase-sensitive detection techniques were utilized, the only effect of these metastables in the proton beam was to increase the background signal. The prequench field was observed to have no effect on the focus of the proton beam. Field penetration into the interaction region which would produce a residual electric field was determined by measuring the modulated photon signal as a function of prequench field voltage. No increase was observed for prequench voltages up to 2300 V.

IV. EXPERIMENTAL PROCEDURE

A preliminary check was made to ascertain that the direct-excitation signals did indeed saturate at low quench voltages. In order to eliminate the charge-transfer process, a He⁺ beam was used in place of the proton beam so that only the target H atoms could be excited with subsequent emission of Lyman- α radiation. Measurements taken for target beams of atomic and molecular hydrogen as well as deuterium showed saturation of the metastable signals at quench voltages of 300 V and above. The saturation of charge-transfer signals was confirmed by saturation of the total metastable signals in proton-hydrogen collisions.

The data for proton collisions with hydrogen molecules were gathered first. Photon signals were accumulated for three periods of 200 sec at each V_q . Data were collected in this way at zero quench field, finite field, field reversed, and zero field again. The quenched metastable signals obtained with the field on and then reversed in direction agreed to within their statistical uncertainties. The repeatability of the signals at zero quench field was necessary for the data to be accepted. The proton beam was monitored to ensure a constancy to within 1%.

For the atomic hydrogen case, the procedure was to repeat the measurements for hydrogen molecules at a few selected values of V_q . Then an atomic beam was produced by heating up the furnace and the dissociation fraction D was measured with the proton beam turned off. When the desired D was obtained, the temperature was measured and the proton beam was generated. Data were collected following the procedure described above for the molecular beam case. At the end of the day, D was measured again. Typical count rates at the proton energy of 25 keV were 10 counts/min at the lowest V_q . A typical measurement is shown in Fig. 4 for 25-keV protons.

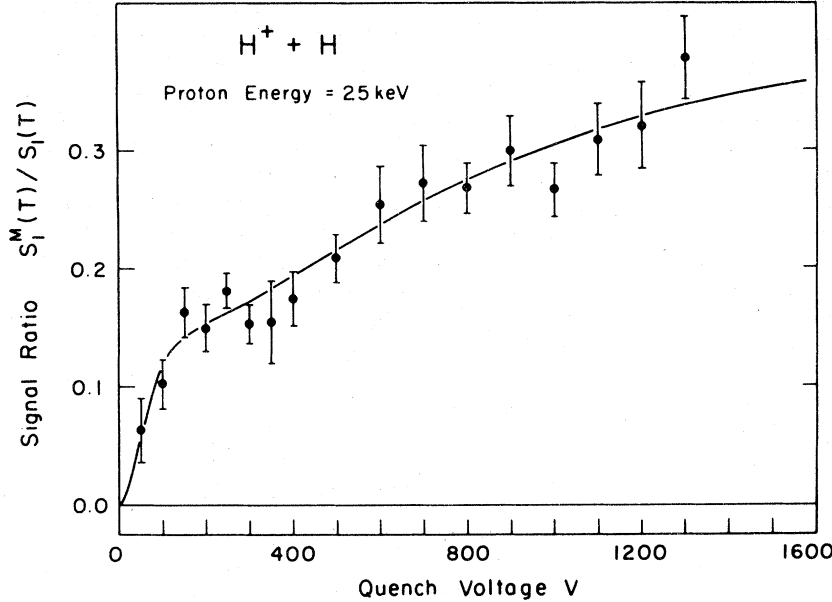


FIG. 4. Photon signal ratio versus quench voltage for collisions of 25-keV protons with hydrogen atoms.

V. DATA ANALYSIS AND CORRECTIONS

A. Quenching efficiency

Since the lifetime $\tau(\xi) = \tau_{2p}$ is the minimum limit attainable and fast metastable atoms produced through charge transfer had a maximum transit time of only 10^{-8} sec, a significant fraction could decay outside the detector's view. However, slow metastables produced through direct excitation remained long enough (10^{-6} sec) within the detector's view for complete quenching to occur when the field strength was adequate. Consider the charge-transfer case. Let $x=0$ and $x=L$ define the width of the rectangular hydrogen beam with the proton beam traveling in the positive x direction. The current $I(x)$ of metastable atoms in the fast beam as a function of x , considering both formation by charge transfer into the metastable state and decay of the metastable atoms by quenching, is given by

$$I(x) = I_p n_H Q_{90}^c v \tau (1 - e^{-x/v\tau}), \quad 0 \leq x \leq L$$

$$= I(L) e^{-(x-L)/v\tau}, \quad x > L \quad (6)$$

where I_p is the proton beam current in ions/sec, n_H , the hydrogen-atom number density, Q_{90}^c the apparent cross section for charge transfer, v the velocity of the fast metastable atoms, and τ is dependent on E_q through Eqs. (3) and (4). The total number of quenched photons emitted within the detector's field of view is then

$$\Phi^c = \int_0^{L+d} \frac{I(x)}{v\tau} dx = I_p n_H Q_{90}^c LC(E_q), \quad (7)$$

where

$$C(E_q) = 1 + (v\tau/L)(e^{-(L+d)/v\tau} - e^{-d/v\tau}), \quad (8)$$

where E_q is the quench field and d is the average distance from the edge $x=L$ to the limit of the detector's field of view. For complete quenching, $C(E_q) = 1$. In the present experiment, the fraction $C(E_q)$ of fast H(2S) atoms quenched within the detector's view ranged from 0.61 for 6-keV protons to 0.38 for 25-keV protons. The effect of the highest applied electric field on the proton velocity is less than 0.1% and therefore has been neglected.

The direct-excitation case can be similarly treated. If the proton beam defines the x axis and the neutral beam the y axis, then the circular cross section of the proton beam causes d to vary over the z axis. The total number of photons emitted within the detector's view is

$$\Phi^d = I_p n_H Q_{90}^d LD(E_q), \quad (9)$$

where

$$D(E_q) = 1 - \frac{v\tau}{\pi R^2} \int_{-R}^R (e^{G(z)} - e^{H(z)}) dz, \quad (10)$$

$$G(z) = (1/v\tau)[(R^2 - z^2)^{1/2} - a - (a/b)z], \quad (11)$$

$$H(z) = (1/v\tau)[(R^2 - z^2)^{1/2} + a + (a/b)z]. \quad (12)$$

Here $2R$ is the proton beam diameter, Q_{90}^d the apparent cross section for direct excitation, a the radius of the circular base in the xy plane of the cone forming the detector's field of view, and b the distance of the apex from this base. The integral was numerically integrated. For complete quenching $D(E_q) = 1$. The symmetry in the detection

geometry ensured that the same fraction of photons was detected in both the charge-transfer and direct-excitation cases. Since simultaneous measurements of the H(2S) and H(2P) cross sections were made under the same experimental conditions, the relative signal was proportional to the ratio of the total photon numbers, i.e.,

$$R_1 = A(E)D(E_q) + B(E)C(E_q), \quad (13)$$

where

$$A(E) = Q_{90}^d(2S)/Q^T(2P) \quad (14)$$

and

$$B(E) = Q_{90}^c(2S)/Q^T(2P) \quad (15)$$

are the relative cross sections at a proton kinetic energy E ; $Q^T(2P)$ is the total cross section for exciting the H(2P) state. The experimental curves of R_1 vs V_q were fit by Eq. (13) using the method of least squares with $A(E)$ and $B(E)$ as parameters.

B. Corrections for molecular contributions

In order to correct for the detected radiation emitted by undissociated molecular hydrogen in the atomic beam, the ratio $R_2 = S_2^M(T_0)/S_2(T_0)$ for a target H₂ beam was measured. Under effusive flow conditions in the neutral beam source, the observed overall signal $S^M(T)$ was corrected to yield the desired atomic signal $S_1^M(T)$ by the relation

$$S_1^M(T) = S^M(T) - S_2^M(T_0)(T_0/T)^{1/2}(1-D), \quad (16)$$

where T is the furnace temperature in degrees Kelvin, D the dissociation fraction defined in Eq. (5), and $S_2^M(T_0)$ is the metastable signal for a H₂ beam at a temperature T_0 where $D=0$. T_0 was normally 300 °K in the present experiments. The same equation without the superscript M gives the corrected photon signal $S_1(T)$ arising from excitation of the H(2P) state. The corrections were 10–15% for $S_1(T)$ and 12–18% for $S_1^M(T)$.

Equation (16) is valid only if the cross section for H⁺+H₂ is independent of the internal energy of the molecules. $S_2^M(T_0)$ was measured at room temperature whereas the molecules in the atomic beam were at 2900 °K, and the cross sections for hydrogen molecules at 2900 °K are not readily obtainable. Considering vibrational excitation only, if f_n denotes the fractional number of molecules in the n th vibrational state, then the total cross section Q_2 for emission of Lyman- α radiation from proton impact on a distribution of vibrationally excited molecules is

$$Q_2 = f_0 Q_2^{(0)} + f_1 Q_2^{(1)} + \dots, \quad (17)$$

where $Q_2^{(n)}$ denotes the cross section for a hydrogen molecule in the n th vibrational state. Since

the molecules obey a Maxwell-Boltzmann distribution when they effuse from the furnace, the fractional number of molecules in the first vibrational state ($n=1$) relative to that in the ground vibrational state ($n=0$) is given by

$$f_1/f_0 = e^{-h\nu/kT}, \quad (18)$$

where $h\nu$ ($= 0.5$ eV) is the energy separation of the two vibrational levels,⁴¹ k is the Boltzmann constant, and T is the furnace temperature. At $T=3000$ °K, $f_1/f_0=0.145$. Normalization of the total fractional number to unity yields $f_0=1-e^{-\gamma}$ where $\gamma=h\nu/kT$, and

$$f_n = (1-e^{-\gamma})e^{-n\gamma} \quad (19)$$

to good approximation. States with $n \geq 2$ may be neglected since for the second vibrational state $f_2/f_0=0.02$. Then Eq. (17) becomes

$$Q_2 = (1-e^{-\gamma})(Q_2^{(0)} + e^{-\gamma}Q_2^{(1)}). \quad (20)$$

The molecular signal $S_2(T)$ with $D=0$ can be expressed as

$$S_2(T) = S_2(T_0)(T_0/T)^{1/2}(Q_2/Q_2^{(0)}), \quad (21)$$

where $S_2(T_0)$ is the molecular signal at room temperature T_0 . Using Eq. (20) and taking logarithms,

$$\ln S_2(T) = C - \frac{1}{2} \ln T + \ln(1 - e^{-h\nu/kT}) + \ln[1 + (Q_2^{(1)}/Q_2^{(0)})e^{-h\nu/kT}], \quad (22)$$

where C represents the constant term at T_0 . At low temperatures $Q_2^{(1)}e^{-h\nu/kT}/Q_2^{(0)} \ll 1$, the logarithmic functions can be expanded to obtain

$$\ln S_2(T) \approx C - \frac{1}{2} \ln T + e^{-h\nu/kT}[(Q_2^{(1)}/Q_2^{(0)}) - 1]. \quad (23)$$

If Q_2 changes with temperature, then applying Eq. (16) to correct for molecular contributions introduces an error. The change in Q_2 will cause the $\ln S$ vs $\ln T$ curve to deviate from linearity obtained under the present conditions of effusive flow. An experimental study was made by measuring the photon signal $S_2(T)$ from the molecular beam as T was increased while maintaining $D=0$. Zero dissociation at temperatures up to 2000 °K was achieved by increasing the hydrogen pressure in the furnace but without exceeding the limits of effusive flow. Using the data with the formulas derived in Eqs. (18)–(20), Q_2 was obtained as not more than 11% larger than $Q_2^{(0)}$. The error contributed by using $Q_2^{(0)}$ instead of Q_2 in Eq. (16) does not change the final cross section values by more than 0.5%.

C. Polarization

The angular distribution of the quenched radiation is that of an electric dipole oriented parallel to the electric field so that the actual cross sec-

tions are given by

$$Q(2S) = (1 - \frac{1}{3}P)Q_{90}(2S), \quad (24)$$

where P is the polarization of the Lyman- α radiation emitted from the H(2S) atom when quenched in an external electric field. With the present detector acceptance angle, the effect of Doppler broadening on the emitted radiation is negligible and therefore disregarded. In the present experiment, P is taken as the theoretical value of -0.323 obtained by Casalese and Gerjuoy,⁴² and which compares with the experimental value of -0.30 ± 0.02 measured by Ott *et al.*⁴³ Later measurements of Sellin *et al.*⁴⁴ and Spiess *et al.*⁴⁵ are in close agreement. Although the polarization depends on the manner of entry into the quench field, the correction is only 1.8% when the polarization calculated by Crandall and Jaecks⁴⁶ for the case of sudden entry is used.

D. Cascade contributions

The cross sections measured in this experiment include cascade contributions. According to electric dipole selection rules, the 3P and 4P states are connected to the 2S state. A consideration of their lifetimes and the branching ratios²⁸ shows that only 12% of the H(3P) and H(4P) atoms will yield H(2S) atoms. In the charge-transfer process the relatively long lifetime of the H(3P) atoms results in a maximum of only 18.6% making a transition to the 2S state within the detector's view. Hughes *et al.*⁴⁷ have measured cross sections for production of H(3P) in proton-inert-gas collisions. Assuming that a similar cross section applies to the proton-hydrogen-atom collisions, the cascade contribution is obtained as less than 1.5% above 10 keV. If the cross section values calculated by Band⁴⁸ are taken, the contribution is below 2.2%. In the direct-excitation process, the Glauber approximation calculations of Franco and Thomas²⁰ give cross sections for the H(3P) state. With these values, the cascade contributions are 4% at 6 keV and 12% at 25 keV. Although changes in lifetimes and branching ratios should occur in strong electric fields,²⁸ we have neglected such changes in making these estimates.

E. Normalization

The relative cross sections obtained were normalized to the absolute total cross section $Q^T(2P)$ determined by Kondow *et al.*³² Their values were obtained by normalization to the cross section for $e + H \rightarrow H(2P) + e$ at an electron energy of 1000 eV, which is obtained from the Born approximation as $0.14\pi a_0^2$.⁴⁹

F. Overall uncertainty

The overall uncertainty in the absolute cross sections arises from statistical fluctuations in the individual measurements of the signal ratio R_1 and from uncertainties in the measurements of the dissociation fraction, determination of the quench-field strength, and the reading of current meters. The normalization to the absolute total cross section for Lyman- α emission from the 2P state determined by Kondow *et al.*³² adds an uncertainty of 6%. The total experimental uncertainties in the absolute cross sections for direct excitation were estimated to be 26% at 6 keV, decreasing to 17% at 15 keV except for 46% at 8 keV. For the charge-transfer absolute cross sections the overall uncertainty was 23% at 8 keV and below 21% at other energies. The uncertainties quoted represent one standard deviation each.

VI. RESULTS AND DISCUSSIONS

Figures 5 and 6 show the cross sections, which have not been corrected for cascade contributions, for the direct-excitation and charge-transfer processes, respectively. Error bars for the present results represent one standard deviation and include systematic uncertainties in the measurements of furnace temperature and dissociation fraction as well as statistical fluctuations in the molecular signal. Experimental values from other measurements are also shown for comparison. Theoretical predictions for direct excitation are included in Fig. 5, while for the charge-transfer process, the comparison is shown in Fig. 7.

In the direct-excitation process, the present results show a minimum at 8 keV with increasing values up to 25 keV. The only other measurement of Morgan *et al.* shows a rather different energy dependence; a level curve up to 10 keV with a rapid rise until 16 keV, where it becomes level again, crossing the present curve at about 25 keV. Below 25 keV, Morgan's values are generally higher by a factor of about 2.

For the charge-transfer process, the present cross sections are in satisfactory agreement with the results of Morgan *et al.*²⁷ and Bayfield²⁶ except at 6 keV where their values also differ. The present value at 6 keV is a factor of 2 higher than that of Morgan *et al.* and a factor of 3 over that of Bayfield. The present curve tends towards a less convex slope above 6 keV, rising a sharper maximum at 20 keV in comparison to the other curves.

Morgan *et al.* performed a crossed-beam experiment employing a different experimental approach, while Bayfield used a projectile-furnace-gas target arrangement. Bayfield normalized his relative cross sections at each proton energy to his abso-

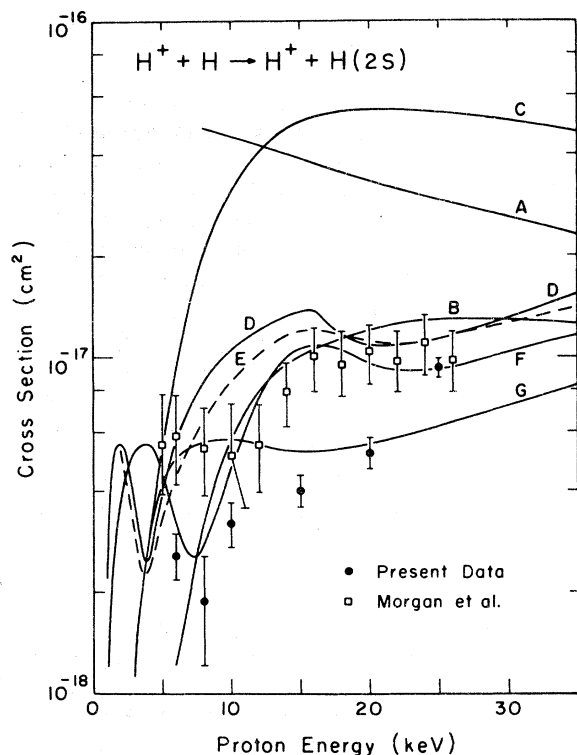


FIG. 5. Cross sections $Q^d(2S)$ for direct excitation in proton collisions with atomic hydrogen. Experimental: \bullet , present data; \square , Morgan *et al.* Theoretical: Curve A, Born (Bates and Griffing); curve B, distortion (Bates); curve C, four-state close coupling without exchange (Flannery); curve D, four-state close coupling with exchange (Cheshire *et al.*); curve E, seven-state close coupling with exchange (Rapp and Dinwiddie); curve F, seven-state pseudostate close coupling (Cheshire *et al.*); curve G, Glauber (Franco and Thomas).

lute measurements⁵⁰ of the capture cross section into the H(2S) state for proton-argon collisions.

The apparent discrepancies in the direct-excitation cross section results of Morgan *et al.* with the present measurement warrant further discussion. Morgan *et al.* detected the photon signals at angles of 90° and 54.7° . They used an oxygen filter of about 0.4 cm in length which allowed 75.6% of the unshifted Lyman- α radiation to be transmitted at 90° . At 54.7° the Doppler-shifted radiation transmitted through the filter was 35% at 6 keV, 20% at 10 keV and 6% at 20 keV as measured by them. Thus a considerable portion of the charge-transfer signal was detected at 54.7° . Since the charge-transfer cross section is large compared to the direct-excitation signal at low energies, the contributions to the total signal at 54.7° of the transmitted charge transfer radiation were comparable to the direct-excitation signal. Small errors in the transmission of the large signal

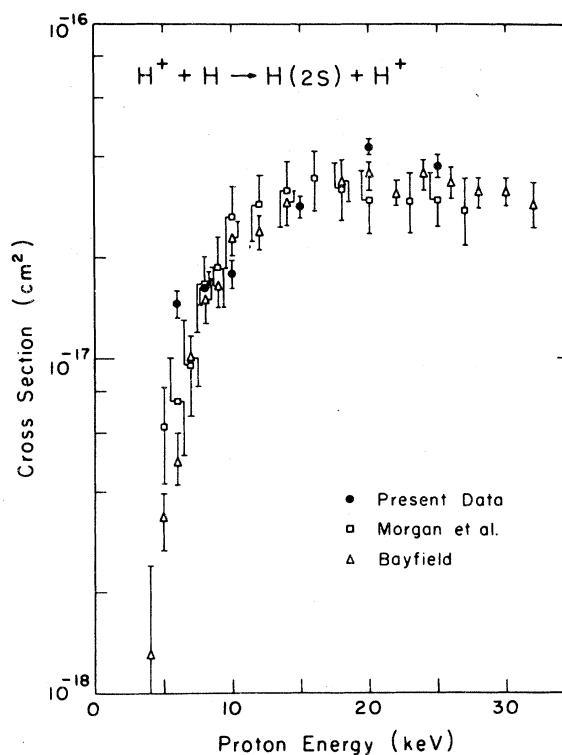


FIG. 6. Cross sections $Q^c(2S)$ for charge transfer in proton collisions with atomic hydrogen: \bullet , present data; \square , Morgan *et al.*; \triangle , Bayfield.

could lead to large errors in the estimation of the direct-excitation signal. In the present experiment measurements were made at 90° only so that the question of the Doppler-shifted radiation does not enter. We suggest that the difference in shape of the direct-excitation cross section may arise in part from inaccuracy of the transmission of the filter that Morgan *et al.* used. On the other hand, an error may exist in the present determination of the low direct-excitation cross section.

With regards to the absolute magnitude, it is noted that the results of Morgan *et al.* depended upon (1) an absolute measurement of the NO photoionization cross section by Lyman- α radiation made by Watanabe *et al.*,⁵¹ (2) the measurement by Andreev *et al.*⁵² using a NO photoionization chamber as the Lyman- α detector in an absolute measurement of the cross section for $H^+ + Ne \rightarrow H(2P) + Ne^+$, (3) the cross-section measurement for $H^+ + H_2 \rightarrow H(2P) + H_2^+$ by Birely and McNeal,⁵³ who normalized their data to that of Andreev *et al.*,⁵² (4) the cross-section measurement by Morgan *et al.* for $H^+ + H \rightarrow H^+ + H(2P)$ and $H^+ + H \rightarrow H(2P) + H^+$ using Birely and McNeal's absolute value, and (5) the measurement of cross sections for H(2S) production.

In the present experiment the starting point was

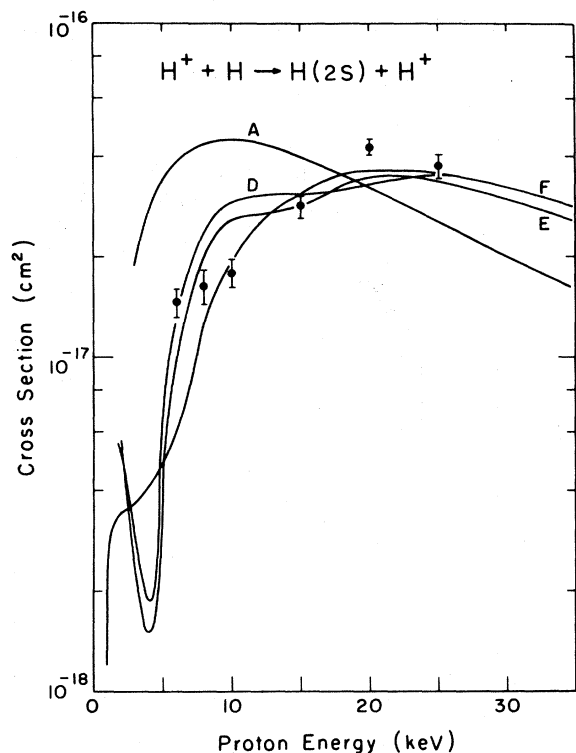


FIG. 7. Comparison of present results with theoretical calculations of the charge-transfer cross section: ●, present data; curve A, Born (Bates and Dalgarno); curve D, four-state close coupling with exchange (Cheshire *et al.*); curve E, seven-state close coupling with exchange (Rapp and Dinwiddie); curve F, seven-state pseudostate close coupling with exchange (Cheshire *et al.*).

(1) the assumption of the validity of the Born approximation for the excitation of Lyman- α radiation in $e + H$ collisions, then (2) the measurement by Kondow *et al.*³² of the ratio of the cross section for $H^+ + H \rightarrow H^+ + H(2P)$ plus $H^+ + H \rightarrow H(2P) + H^+$ to the electron-impact excitation cross section, and (3) the present experiment.

The cumulative uncertainties of the various measurements leading to the results of Morgan *et al.* are estimated by them to be $\pm 30\%$. A slightly less uncertainty would accrue to the present measurements. The actual differences in the values of the measured sums of Q_d and Q_e in the results

of Morgan *et al.* and the present experiment fall within the combined uncertainties of both experiments.

The theoretical values of Cheshire *et al.*¹¹ from the pseudostate expansion (Figs. 5 and 7, curve F) show better agreement with the present data than their hydrogenic calculations shown by curve D (four-state expansion as well as the hydrogenic calculations of Rapp and Dinwiddie¹⁶ shown by curve E (seven-state expansion). For the direct-excitation process, the pseudostate calculation shows a minimum similar to, but higher by a factor of 1.4, than that in the present curve at about 8 keV. The maximum in curve F at 15 keV was not observed, but the theoretical value at 25 keV coincides with the present value. In the charge-transfer cross section, the results of Cheshire *et al.* show the maximum at 20 keV seen in the present measurement, but below 10 keV the predicted values decrease much faster than was observed.

The Born approximation^{2,3} (Figs. 5 and 7, curve A) shows poor agreement with the present results while the distortion approximation⁵⁴ (Fig. 5, curve B) shows slightly improved values. Curve C represents the four-state close-coupling calculations of Flannery,¹² who neglected exchange. Later predictions of Sullivan *et al.*¹³ and Baye and Heenen¹⁷ are in close agreement with curve C, but all three disagree with the present results. The Glauber approximation^{19,20} shown by curve G exhibits poor agreement in shape although the magnitude is better predicted than from the other calculations besides curve F.

The satisfactory agreement with the pseudostate close-coupling calculations of Cheshire *et al.* demonstrates the importance of the charge-transfer reaction channels and the inclusion of molecular features at small internuclear separations by incorporating pseudostates.

ACKNOWLEDGMENTS

We gratefully acknowledge the continuing interest and expert advice, particularly in technical details, of our colleague Dr. H. H. Lo, and the help of our former colleague, Dr. Tomatsu Kondow, during the earliest parts of this work. The assistance of Jeffrey Halle in taking much of the data is also gratefully acknowledged.

*Research supported by the National Science Foundation under Grant No. MPS74-08174 A01.

†Present address: Department of Physics and Astronomy, University of Maryland, College Park, Md. 20742.

¹J. D. Jackson and H. Schiff, *Phys. Rev.* **89**, 359 (1953).

²D. R. Bates and G. Griffing, *Proc. Phys. Soc. Lond.* **A 66**, 961 (1953).

³D. R. Bates and A. Dalgarno, *Proc. Phys. Soc. Lond.* **A 66**, 972 (1953).

⁴D. R. Bates, *Proc. R. Soc. Lond.* **A 245**, 299 (1958).

⁵R. A. Mapleton, *Phys. Rev.* **126**, 1477 (1962).

⁶M. B. McElroy, *Proc. R. Soc. Lond.* **272**, 542 (1963).

⁷D. R. Bates, *Proc. Phys. Soc. Lond.* **73**, 227 (1959).

⁸J. P. Coleman and M. R. C. McDowell, *Proc. Phys. Soc. Lond.* **85**, 1097 (1965).

- ⁹D. R. Bates, Proc. R. Soc. Lond. A 247, 294 (1958).
¹⁰S. E. Lovell and M. B. McElroy, Proc. R. Soc. Lond. A 283, 100 (1965).
¹¹I. M. Cheshire, D. F. Gallagher, and A. J. Taylor, J. Phys. B 3, 813 (1970).
¹²M. R. Flannery, J. Phys. B 2, 1044 (1969).
¹³J. Sullivan, J. P. Coleman, and B. H. Bransden, J. Phys. B 5, 2061 (1972).
¹⁴B. H. Bransden, J. P. Coleman, and J. Sullivan, J. Phys. B 5, 546 (1972).
¹⁵D. Rapp, D. Dinwiddie, D. Storm, and T. E. Sharp, Phys. Rev. A 5, 1290 (1972).
¹⁶D. Rapp and D. Dinwiddie, J. Chem. Phys. 57, 4919 (1972).
¹⁷D. Baye and P. H. Heenen, J. Phys. B 6, 105 (1973).
¹⁸J. P. Coleman, J. Phys. B 1, 567 (1968).
¹⁹A. S. Ghosh and N. C. Sil, J. Phys. B 4, 836 (1971).
²⁰V. Franco and B. K. Thomas, Phys. Rev. A 4, 945 (1971).
²¹F. W. Byron, Jr., Phys. Rev. A 4, 1907 (1971).
²²C. J. Joachain and R. Vanderpoorten, J. Phys. B 6, 622 (1973).
²³Y. B. Band, Phys. Rev. A 8, 243 (1973).
²⁴D. Storm, Phys. Rev. A 8, 1765 (1973).
²⁵G. Ryding, A. B. Wittkower, and H. B. Gilbody, Proc. Phys. Soc. Lond. 89, 547 (1966).
²⁶J. E. Bayfield, Phys. Rev. 185, 105 (1969).
²⁷T. J. Morgan, J. Geddes, and H. B. Gilbody, J. Phys. B 6, 2118 (1973).
²⁸H. A. Bethe and E. E. Salpeter, *Quantum Mechanics of One- and Two-Electron Atoms* (Academic, New York, 1957).
²⁹I. A. Sellin, Phys. Rev. 136, A1245 (1964).
³⁰J. Shapiro and G. Breit, Phys. Rev. 113, 179 (1959).
³¹W. E. Kauppila, P. J. O. Teubner, W. L. Fite, and R. J. Girnius, Phys. Rev. A 2, 1759 (1970).
³²T. Kondow, R. J. Girnius, Y. P. Chong, and W. L. Fite, Phys. Rev. A 10, 1167 (1974).
³³K. Watanabe, Adv. Geophys. 5, 153 (1968).
³⁴M. Ogawa, J. Geophys. Res. 73, 6759 (1968).
³⁵T. D. Gaily, J. Opt. Soc. Am. 59, 536 (1969).
³⁶J. D. Carriere and F. J. de Heer, J. Chem. Phys. 56, 2993 (1972).
³⁷P. Lee, J. Opt. Soc. Am. 45, 763 (1955).
³⁸W. E. Lamb, Jr., and R. C. Retherford, Phys. Rev. 79, 549 (1950); 81, 222 (1951).
³⁹R. T. Robiscoe, Phys. Rev. 138, A22 (1965).
⁴⁰W. L. Fite, R. T. Brackmann, D. G. Hummer, and R. F. Stebbings, Phys. Rev. 116, 363 (1959).
⁴¹G. Herzberg, *Spectra of Diatomic Molecules* (Van Nostrand, New York, 1950).
⁴²J. Casalese and E. Gerjuoy, Phys. Rev. 180, 327 (1969).
⁴³W. R. Ott, W. E. Kauppila, and W. L. Fite, Phys. Rev. A 1, 1089 (1970).
⁴⁴I. A. Sellin, J. A. Biggerstaff and P. M. Griffin, Phys. Rev. A 2, 423 (1970).
⁴⁵G. Spiess, A. Valance, and P. Pradel, Phys. Rev. A 6, 746 (1972).
⁴⁶D. H. Crandall and D. H. Jaacks, Phys. Rev. A 4, 2271 (1971).
⁴⁷R. H. Hughes, C. A. Stigers, B. M. Doughty, and E. D. Stokes, Phys. Rev. A 1, 1424 (1970).
⁴⁸Y. B. Band, Phys. Rev. A 8, 2857 (1973).
⁴⁹H. S. W. Massey and E. H. S. Burhop, *Electronic and Impact Phenomena* (Clarendon, New York, 1952), p. 170.
⁵⁰J. E. Bayfield, Phys. Rev. 182, 115 (1969).
⁵¹K. Watanabe, F. M. Matsunaga, and H. Sakai, Appl. Opt. 6, 391 (1967).
⁵²E. P. Andreev, V. A. Ankudinov, and S. V. Bobashev, Zh. Eksp. Teor. Fiz. 50, 565 (1966) [Sov. Phys. JETP 23, 375 (1966)].
⁵³J. H. Birely and R. J. McNeal, Phys. Rev. A 5, 692 (1972).
⁵⁴D. R. Bates, Proc. Phys. Soc. Lond. 77, 59 (1961).